Generating maximally-path-entangled number states in two spin ensembles coupled to a superconducting flux qubit

Yusef Maleki[1,*] and Aleksei M. Zheltikov[1,2,3,4,5]

[1]*Department of Physics and Astronomy, Texas A&M University, College Station, Texas 77843-4242, USA*
[2]*Physics Department, International Laser Center, M. V. Lomonosov Moscow State University, Moscow 119992, Russia*
[3]*Russian Quantum Center, ul. Novaya 100, Skolkovo, Moscow Region 143025, Russia*
[4]*Kurchatov Institute National Research Center, Moscow 123182, Russia*
[5]*Kazan Quantum Center, A.N. Tupolev Kazan National Research Technical University, 420126 Kazan, Russia*

(Received 27 September 2017; published 16 January 2018)

An ensemble of nitrogen-vacancy (NV) centers coupled to a circuit QED device is shown to enable an efficient, high-fidelity generation of high-N00N states. Instead of first creating entanglement and then increasing the number of entangled particles N, our source of high-N00N states first prepares a high-N Fock state in one of the NV ensembles and then entangles it to the rest of the system. With such a strategy, high-N N00N states can be generated in just a few operational steps with an extraordinary fidelity. Once prepared, such a state can be stored over a longer period of time due to the remarkably long coherence time of NV centers.

DOI: 10.1103/PhysRevA.97.012312

I. INTRODUCTION

Phase measurements play the central role in the quest for ultimate precision in science and technology with a span of applications from gravity-wave detection [1] to superresolving microscopy on the nanoscale [2]. The fundamental shot-noise limit (SNL) that classical physics sets on the precision of such measurements scales as $1/\sqrt{N}$ with N being the number of times that the studied system is sampled during a measurement. Quantum correlations help overcome this limit [3], opening the ways toward phase superresolution in atomic frequency measurements [4], interferometry [5], and quantum lithography [6].

As one of the most prominent examples, the N00N states [6,7] $(e^{i\phi}|N\rangle_a \otimes |0\rangle_b + |0\rangle_a \otimes |N\rangle_b)/\sqrt{2}$, representing a Fock-state superposition of N quantum particles that are all either in the a or in the b mode of the system, can provide quantum probes that reach the $1/N$ Heisenberg limit (HL) of precision in phase measurements [8,9]. In experiments, N00N states can be generated through a delicate manipulation of quantum states of light [10,11], as well as by using circuit QED systems [12,13] such as superconducting qubits coupled to microwave cavities [14], or in spin ensembles [15]. As a breakthrough achievement, 10-spin N00N states have been generated using nuclear spins in a molecule [15].

Many of the recently proposed fast and elegant methods of high-N00N state generation [16,17] start with an $N = 1$ entangled-state preparation to proceed with a step-by-step increase in N in this state. Each such step, however, leads to a buildup of decoherence, which dramatically lowers the efficiency N00N-state generation and the fidelity of high-N00N output [17].

Here we present a method of high-N N00N-state generation that allows this excessive fidelity loss to be avoided. We show that high-N N00N states can be generated using quantum memories based on ensembles of nitrogen-vacancy (NV) centers interacting with a superconducting flux qubit. In our scheme, instead of first creating entanglement and then increasing N, we first prepare a high-N Fock state in one of the NV center ensembles (NVEs) and then entangle it to the rest of the system. With such a strategy, high-N N00N states can be generated in just a few operational steps with a high fidelity and high immunity to decoherence. We demonstrate that, once prepared, such a state can be stored over a longer period of time due to the remarkably long coherence time of NV centers.

II. THE MODEL

We consider a quantum structure consisting of two separate noninteracting diamond NVEs coupled to a common large superconducting gap-tunable flux qubit [Fig. 1(a)] [18,19]. Such a hybrid structure combines the long-lived coherence of spins in NV centers, the capability of controlling NV center by microwave and optical fields [20–22], the tunability of superconducting devices, circuit scalability, and compatibility with cutting-edge nanotechnologies [18,23,24]. Unlike microwave photons in superconducting cavities, which have lifetimes on the order of 1 ms [25], the coherence time of NV centers can approach 1 s even at moderately high temperatures [26], offering a unique platform for quantum memories [27].

With the biasing in the main loop close to half the flux quantum, $\Phi_0 = h/(2e)$, with h being the Planck constant and e the electron charge, the flux qubit can be described [19,24] in terms of a two-level Hamiltonian $H = -[\epsilon(\Phi_{\rm ext})\sigma_z + \Delta(\Phi'_{\rm ext})\sigma_x]/2$, where σ_x and σ_z are the Pauli operators in the basis of flux qubit, $\Delta(\Phi'_{\rm ext})$ is the qubit tunneling splitting energy, and $\epsilon(\Phi_{\rm ext})$ is the energy bias of the flux qubit. With a static magnetic field of half the flux quantum applied perpendicular to the main loop of the flux qubit, the clockwise and counterclockwise persistent current states in the system are almost degenerate [24,28]. We can thus define the logical basis

*Corresponding author: maleki@physics.tamu.edu

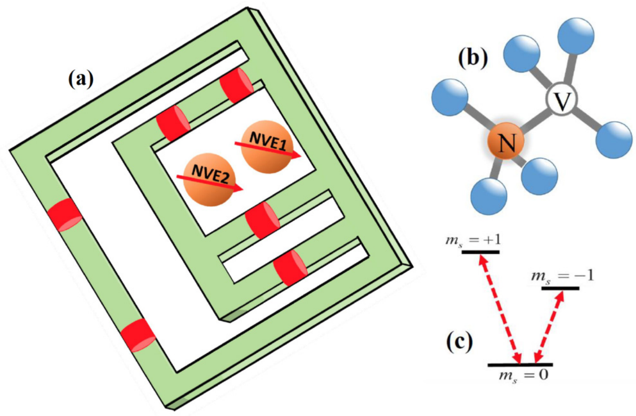

FIG. 1. (a) Two ensembles of NV centers coupled to a superconducting flux qubit consisting of four Josephson junctions forming the main loop and an α loop. (b, c) Crystal-lattice (b) and energy (c) diagrams of an NV center in diamond.

states $|0\rangle_f$ and $|1\rangle_f$ as the states of the clockwise and counterclockwise persistent current, respectively. Since $\epsilon(\Phi_{\rm ext})$ and $\Delta(\Phi'_{\rm ext})$ can be controlled independently by external magnetic fluxes through the main and the α loops, we can set $\epsilon(\Phi_{\rm ext}) = 0$.

The ground state of an NV center is a spin triplet with zero-magnetic-field splitting $D_{gs} \approx 2.87$ GHz between the $m_s = 0$ sublevel and and the degenerate $m_s = \pm 1$ sublevels [Figs. 1(b) and 1(c)]. An external magnetic field $B_{\rm ext}$ applied along the [100] direction of the diamond crystal lattice induces Zeeman splitting, removing the degeneracy of $|m_s = \pm 1\rangle$ sublevels [Fig. 1(c)]. In the presence of an ac microwave magnetic field B_j whose magnitude is small compared to $B_{\rm ext}$, the spin operators of the jth NV center are defined as $s_{zj} = |-1_j\rangle\langle -1_j| - |0_j\rangle\langle 0_j|$, $s_{+j} = |-1_j\rangle\langle 0_j|$ and $s_- = |0_j\rangle\langle -1_j|$. For an NVE consisting of N_0 NV centers, collective spin operators can then be written as $S_\tau = \sum_{k=1}^{N_0} s_{\tau k} (\tau = z, \pm)$.

Qubits based on NV centers with an external magnetic field $B_{\rm ext}$ applied to induce splitting between the $m = 0$ and $m = -1$ sublevels have been examined in the extensive earlier work (see, e.g., Refs. [24,28,29]). As a significant distinction, the method of N00N state generation proposed here involves additional time-dependent B_j fields, applied to NVEs along with $B_{\rm ext}$ to provide a periodic modulation of the $m = 0$ – $m = -1$ splitting. As an important step of our analysis, we extend the Holstein-Primakoff (HP) transformation [30] to the spin operators of NV centers with time-dependent $m = 0$ – $m = -1$ splitting and show that such a transformation leads to a closed-form Hamiltonian [Eq. (1) below], facilitating the analysis of N00N-state generation in such a system.

In the regime of weak excitation, the spin operators of an NVE with large N_0 can be mapped onto bosonic operators via an HP transformation [30], $\sum_{k=1}^{N_0} s_{+k}^j = c_j^\dagger \sqrt{N_0 - c_j^\dagger c_j} \simeq \sqrt{N_0} c_j^\dagger$, $\sum_{k=1}^{N_0} s_{-k}^j = c_j \sqrt{N_0 - c_j^\dagger c_j} \simeq \sqrt{N_0} c_j$, and $\sum_{k=1}^{N_0} s_{zk}^j = 2 c_j^\dagger c_j - N_0$, where $j = 1{,}2$ for the first and the second NVEs, respectively, and $[c_j, c_j^\dagger] = 1$. The coupling strength of an ensemble of N_0 spins is thus enhanced by a factor of $\sqrt{N_0}$ compared to the coupling strength of a single spin [31,32]. The weak-excitation requirement, necessary for the validity of HP mapping, is satisfied when $c_1^\dagger c_1 \ll N_0$ and $c_2^\dagger c_2 \ll N_0$. This limits the N number in attainable N00N states, $N \ll N_0$. Specifically, with $N_0 \sim 10^7$ [23], the HP map will become invalid for $N \gtrsim 10^6$.

The total Hamiltonian of the NVE-flux-qubit hybrid system considered here can now be written as

$$H = -\hbar \frac{\Delta(\Phi'_{\rm ext})}{2} \sigma_x + \hbar \sum_{j=1}^{2} \omega_j c_j^\dagger c_j + \hbar \sum_{j=1}^{2} g (c_j^\dagger + c_j) \sigma_z, \tag{1}$$

where $\omega_j = D_{gs} - g_e \mu_B B_z - g_e \mu_B B_j$, g_e is the ground-state Lande factor, μ_B is the Bohr magneton, B_z is the magnetic field sensed by the spins due to the applied external magnetic filed $B_{\rm ext}$ and the magnetic field produced by the flux qubit, and g is the constant quantifying the coupling between the NVE ensembles and the flux qubit.

We assume that the sizes of the NVEs are sufficiently small to neglect spatial variations of the magnetic field induced by the flux qubit. Furthermore, the magnetic fields are chosen such that $\omega_j = \Delta(\Phi'_{\rm ext})/2 + \delta \sin(\nu t + \varphi_j)$, where $\delta \sin(\nu t + \varphi_j)$ is controlled by the ac magnetic field. Choosing large ν and small δ, so that $\Delta(\Phi'_{\rm ext}) \gg \zeta = \delta/\nu$, we apply the rotating-wave approximation and use the basis of flux qubit eigenstates to reduce the interaction Hamiltonian of the considered system [33] to

$$H_I = \hbar g \sigma^+ (\hat{c}_1 e^{i\zeta \cos(\nu t + \varphi_1)} + \hat{c}_2 e^{i\zeta \cos(\nu t + \varphi_2)}) + {\rm H.c.} \tag{2}$$

This Hamiltonian can be reduced to a Floquet Hamiltonian by using the identity $e^{i\zeta \cos(\nu t + \varphi_j)} = \sum_{n=-\infty}^{\infty} J_n(\zeta) e^{in(\nu t + \varphi_j)}$, where $J_n(\zeta)$ is the nth-order Bessel function of the first kind, which gives $H_I = H_0 + \sum_{n=1}^{\infty} H_n e^{in\nu t}$, where $H_0 = \hbar g J_0(\zeta)[\sigma^+(\hat{c}_1 + \hat{c}_2) + (\hat{c}_1^\dagger + \hat{c}_2^\dagger)\sigma^-]$ and $H_n = \hbar g \sum_{j=1}^{2} i^n J_n(\zeta)[\sigma^+ \hat{c}_j + (-1)^n \hat{c}_j^\dagger \sigma^-] e^{in\varphi_j}$. The interaction Hamiltonian of this form can be replaced [34,35] by the effective Hamiltonian $H_{\rm eff} = H_0 + \sum_{n=1}^{\infty} [H_n, H_{-n}]/(n\hbar\nu)$, which can be written as [33–36] $H_{\rm eff} = \hbar g J_0(\zeta)[\sigma^+(\hat{c}_1 + \hat{c}_2) + {\rm H.c.}] + i\hbar\Omega(\hat{c}_1^\dagger \hat{c}_2 - \hat{c}_1 \hat{c}_2^\dagger)\sigma_z$. Here $\Omega = g^2\chi/\nu$ is the coupling coefficient with $\chi = \sum_{n=1}^{\infty} 2 J_n(\zeta)^2 \sin[n(\varphi_1 - \varphi_2)]/n$.

We set $\zeta = 2.40$ $[J_0(2.40) = 0]$ and $\varphi_2 \neq \varphi_1$ to find the effective interaction Hamiltonian:

$$H_{\rm eff} = i\hbar\Omega(\hat{c}_1^\dagger \hat{c}_2 - \hat{c}_2^\dagger \hat{c}_1)\sigma_z. \tag{3}$$

It is straightforward to see now that the coupling coefficient can be tuned by varying the B_j fields. In particular, with $\varphi_1 - \varphi_2 = \pi/3$ and $\nu = 5\chi g \simeq 3.14 g$, we have $\Omega/2\pi \approx 14$ MHz. Such coupling strengths have been recently demonstrated for a system of a flux qubit and an NVE with $N_0 \approx 3 \times 10^7$ [23]. With the decay rates of NVEs and the flux qubit estimated as $\gamma_{NV} \sim 1$ Hz [26] and $\gamma_{FQ} \sim 1$ MHz [29], we find that the requirement of strong coupling, $\Omega \gg \gamma_{FQ}, \gamma_{NV}$, is fulfilled.

III. N00N STATE GENERATION

We are going to show now that, starting with this interaction Hamiltonian, we can create a N00N state in the NVE memories. To this end, we prepare the superconducting flux qubit in the state $\frac{1}{\sqrt{2}}(|0\rangle_f + |1\rangle_f)$. The first and the second NVEs are

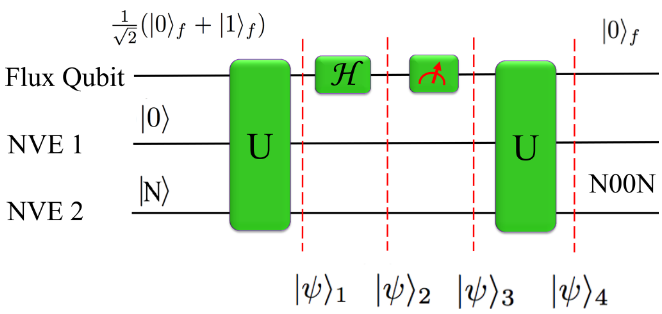

FIG. 2. N00N state generation in NVE memories: U, time evolution of a quantum state, governed by the time-evolution operator $U(t) = e^{-iH_{\rm eff}\Delta t/\hbar}$ with the effective Hamiltonian $H_{\rm eff}$; $\mathcal{H}$, an Hadamard gate acting locally on the flux qubits. Within the time interval $\Delta t_1 = \pi/(4\Omega)$, the system evolves from its specifically tailored initial state to $|\psi\rangle_1$. The Hadamard transform yields the state $|\psi\rangle_2$. Upon a measurement on the state of the flux qubit, the total wave function of the systems collapses to $|\psi\rangle_3$. At the final step, time evolution $U(t)$ creates the desired N00N state.

prepared in the $|0\rangle_{c_1}$ and $|N\rangle_{c_2}$ Fock states, respectively. The initial state of the entire system is thus given as $|\psi(0)\rangle = \frac{1}{\sqrt{2}}(|0\rangle_f + |1\rangle_f)|0\rangle_{c_1}|N\rangle_{c_2}$.

Applying the evolution operator $U(t) = e^{-iH_{\rm eff}\Delta t/\hbar}$ to this initial state (Fig. 2), we find

$$|\psi(t)\rangle = \frac{1}{\sqrt{2}}(e^{-iH_{\rm eff}\Delta t/\hbar}|0,N\rangle|0\rangle_f + e^{-iH_{\rm eff}\Delta t/\hbar}|0,N\rangle|1\rangle_f), \tag{4}$$

where $|0,N\rangle \equiv |0\rangle_{c_1}|N\rangle_{c_2}$.

Following evolution within the time interval $\Delta t_1 = \pi/(4\Omega)$, $\Omega > 0$, $|\psi(t)\rangle$ becomes

$$|\psi\rangle_1 = \frac{1}{\sqrt{2^N}}\sum_{k=1}^{N}\binom{N}{k}^{\frac{1}{2}}|k,N-k\rangle(|0\rangle_f + (-1)^k|1\rangle_f). \tag{5}$$

As a next step, we apply an Hadamard gate [37]

$$\mathcal{H} = \frac{1}{\sqrt{2}}\begin{pmatrix}1 & 1\\ 1 & -1\end{pmatrix} \tag{6}$$

to the flux qubit (Fig. 2). This yields a local transformation of the flux-qubit basis $|0\rangle_f \rightarrow \frac{1}{\sqrt{2}}(|0\rangle_f + |1\rangle_f)$, $|1\rangle_f \rightarrow \frac{1}{\sqrt{2}}(|0\rangle_f - |1\rangle_f)$ and transforms, within the time interval Δt_2, the quantum state of our system to

$$|\psi\rangle_2 = \frac{1}{\sqrt{2^N}}\sum_{k=1}^{N}\binom{N}{k}^{\frac{1}{2}}[1 + (-1)^k]|k,N-k\rangle|0\rangle_f + \frac{1}{\sqrt{2^N}}\sum_{k=1}^{N}\binom{N}{k}^{\frac{1}{2}}[1 - (-1)^k]|k,N-k\rangle|1\rangle_f. \tag{7}$$

We now need to perform a measurement on the flux qubit, e.g., by using a SQUID magnetometer attached to the flux qubit [the largest loop in Fig. 1(a)]. The voltage state of such a detector is known to be extremely sensitive to tiny flux variations, allowing the switching between the eigenstates of the flux-qubit Hamiltonian to be detected [19,23]. If the outcome of the measurement performed on the state of the flux qubit within time interval Δt_3 gives $|0\rangle_f$, the wave function of the system collapses to

$$|\psi\rangle_3 = \frac{1}{\sqrt{2^N}}\sum_{k=1}^{N}\binom{N}{k}^{\frac{1}{2}}[1 + (-1)^k]|k,N-k\rangle|0\rangle_f. \tag{8}$$

If, on the other hand, the outcome of the measurement is $|1\rangle_f$, then the wave function of the system is

$$|\psi\rangle_3 = \frac{1}{\sqrt{2^N}}\sum_{k=1}^{N}\binom{N}{k}^{\frac{1}{2}}[1 - (-1)^k]|k,N-k\rangle|1\rangle_f. \tag{9}$$

Now, applying the time-evolution operator once again we can create the N00N state. If the outcome of the measurement is $|0\rangle_f$, then the evolution of the system within a time interval $\Delta t_4 = \pi/(4\Omega)$ past the measurement step (Fig. 2) yields a N00N state in the NVEs:

$$|\text{N00N}\rangle = \frac{1}{\sqrt{2}}[(-1)^N|N\rangle_{c_1}\otimes|0\rangle_{c_2} + |0\rangle_{c_1}\otimes|N\rangle_{c_2}]. \tag{10}$$

If, on the opposite, the outcome of the measurement is $|1\rangle_f$, then, letting the system evolve within a time interval $\Delta t_4 = 3\pi/(4\Omega)$ following the measurement step (Fig. 2), we arrive at the following N00N state in the NVEs:

$$|\text{N00N}\rangle = \frac{1}{\sqrt{2}}(|N\rangle_{c_1}\otimes|0\rangle_{c_2} - |0\rangle_{c_1}\otimes|N\rangle_{c_2}). \tag{11}$$

Remarkably, regardless of the outcome of the measurement on the flux qubit, a N00N state is generated at the final step of our procedure, implying 100% fidelity of N00N state generation from $|\psi\rangle_2$ provided that the measurement is perfect. If the measurement yields $|0\rangle_f$, it takes the system less time to evolve to the N00N state.

As one of its key advantages, our procedure of N00N-state generation requires only local operations on the flux qubit at the second and third steps, at which the state $|\psi\rangle_1$ is transformed into $|\psi\rangle_3$. As a result, the operation time at each of these two steps is reduced to the single-qubit operation time, Δt_2, $\Delta t_3 \sim 1$ ns [28], allowing the overall time $\Delta\tau = \sum_{i=1}^{4}\Delta t_i$ of N00N-state generation to be radically decreased. This is central to avoiding decoherence buildup in the system, which is dominated, at the state of N00N-state generation, by the dephasing of the flux qubit. With our above estimate of $\Omega/2\pi \simeq 14$ MHz, ensuring a strong-coupling regime, we have $\Delta t_1 \approx 9$ ns. Thus, we find that the total time required to create a N00N state through the considered process is $\Delta\tau \approx 20$ ns when the $|0\rangle_f$ state is reached at the measurement step and $\Delta\tau \approx 38$ ns if the measurement step yields $|1\rangle_f$. In both cases, the time required for N00N-state generation is much shorter than the dephasing times of both the flux qubit, $\sim 1\ \mu$s [29], and the NVEs $\sim 350\ \mu$s [38].

The method of N00N state generation proposed here is instrumental in preventing the buildup of decoherence, which may have a damaging effect on N00N states in schemes where such states are generated in the reverse order: via entangled-state creation at the first stage, followed by a step-by-step increase in N in this entangled state which results in more operational steps. The generated N00N state is more robust to decoherence compared to many physical systems. To quantify the buildup of decoherence in the generated N00N state in

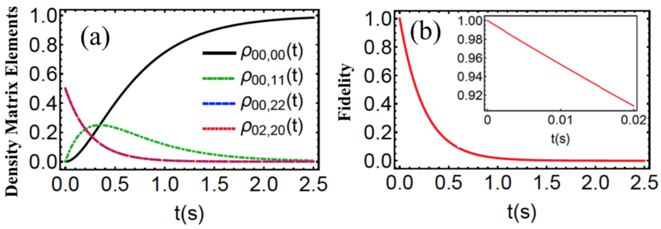

FIG. 3. Time evolution of the density matrix elements $\rho_{ij,kl}$ (a) and the fidelity (b) calculated by solving Eq. (12) for the NVE-flux-qubit source of N00N states with an $N = 2$ N00N state prepared in a system at $t = 0$.

our scheme, we solve the pertinent evolution equation for the density operator $\hat{\rho}$ [39],

$$\frac{\partial \hat{\rho}}{\partial t} = \sum_j -i\omega_j[c_j^\dagger c_j,\hat{\rho}] + \frac{\gamma_j}{2}(1+\bar{n}_{th})(2\hat{c}_j\hat{\rho}\hat{c}_j^\dagger - \hat{c}_j{}^\dagger\hat{c}_j\hat{\rho} - \hat{\rho}\hat{c}_j^\dagger\hat{c}_j) + \frac{\gamma_j}{2}\bar{n}_{th}(2\hat{c}_j^\dagger\hat{\rho}\hat{c}_j - \hat{c}_j\hat{c}_j^\dagger\hat{\rho} - \hat{\rho}\hat{c}_j\hat{c}_j^\dagger), \tag{12}$$

where $j = 1,2$, γ_i is the decoherence rate of the ith NVE, and $\bar{n}_{th} = [\exp(\hbar\omega/k_BT) - 1]^{-1}$ is the thermal excitation number at temperature T with the frequency of ω. After the state is generated, the magnetic field is turned off, and thus we have $\omega = \omega_j = 2.87$ GHz.

In our analysis, we take $\gamma_1 = \gamma_2 = \gamma$ and set $T = 20$ mK. At this temperature, we take $1/\gamma \approx 1$ s as an attainable coherence time for NV centers [26]. In Fig. 3(a) we present the density matrix elements $\rho_{ij,kl} = \langle ik|\hat{\rho}(t)|jl\rangle$ (where $|jl\rangle = |j\rangle_1 \otimes |l\rangle_2$) calculated by numerically solving Eq. (12) with the initial conditions corresponding to an $N = 2$ N00N state shared by the two spin ensembles at $t = 0$. Decoherence is seen to build up in the system on a time scale of hundreds of milliseconds.

In Fig. 3(b) we present the N00N-state fidelity calculated as $F = \langle N00N|\hat{\rho}(t)|N00N\rangle$. As can be seen from these calculations, for our source of N00N states, at $t = 1$ ms, F is still higher than 0.99. Moreover, it remains above 0.97 within time intervals as long as $t \approx 3.5$ ms [the inset in Fig. 3(b)].

We note that at $T = 20$ mK the average thermal excitation number is about $\bar{n}_{th} = 0.001$; while we can sufficiently cool the system below 10 mK with the current technologies where the thermal excitation number of as small as $\bar{n}_{th} \lesssim 10^{-6}$ can be achieved, implying that we can ignore the effect of thermal excitation. Thus, ignoring the thermal effects (at $T = 0$ K), the exact solution of the master equation for N00N state at time t reads

$$\hat{\rho}(t) = \frac{1}{2}\Bigg[\sum_{n=0}^{N} e^{-\gamma nt}\binom{N}{n}(1-e^{-\gamma nt})^{N-n} \times (|n0\rangle\langle n0| + |0n\rangle\langle 0n|) + e^{-\gamma Nt}(|N0\rangle\langle 0N| + |0N\rangle\langle N0|)\Bigg]. \tag{13}$$

With the exact solution of $\hat{\rho}(t)$ at hand, the ultimate precision of a phase measurement is thus obtained as $\Delta\phi \geqslant e^{\gamma Nt/2}/N$, showing that damping leads to an exponential decrease in the sensitivity of phase measurements. Furthermore, to understand the robustness of our scheme against decoherence we consider the fidelity of the N00N state in the system, which can be calculated as $F = e^{-\gamma Nt}$. The fidelity of the N00N state degrades exponentially. Since the decoherence rate is determined in terms of the coherence time of the system $\gamma = \frac{1}{\tau}$, the long coherence time of the NVE provides an exponential advantage compared to most of the proposed physical systems considered in the literature. For a given N, the fidelity drops to $\sim e^{-1}$ at $\gamma Nt = 1$, where the state is effectively collapsed to the ground state.

Significant factors limiting the performance of quantum information systems based on NV centers include the inhomogeneous broadening of spin ensembles due to magnetic dipolar interactions with the nuclear or excessive electron spins in diamond, as well as decoherence caused by the dipole interaction between the redundant nitrogen spins and NV centers [40,41]. Since the magnetic dipolar interactions inducing excessive inhomogeneous broadening are largely due to the magnetic moment of carbon-13, inhomogeneous broadening due to both these factors is almost completely eliminated when NV diamond is prepared, with the use of the existing cutting-edge technologies [42], from isotopically purified carbon-12 with ultralow concentrations of excessive nitrogen.

While the proposed source of N00N states is compatible with many schemes of superresolving phase measurements [4], supersensitive spectroscopy [11], and subdiffraction quantum lithography [6], it is especially well suited for sub-SNL magnetic-field sensing. Indeed, a weak magnetic field B induces a precession of individual spins in NVEs. As a result of this precession, a spin initially in the superposition state $(|0\rangle + |1\rangle)/\sqrt{2}$ evolves to the state $(|0\rangle + e^{-i\gamma_e Bt}|1\rangle)/\sqrt{2}$ within time t, γ_e being the gyromagnetic ratio. A system of N unentangled spins can thus measure B with a $1/\sqrt{N}$ sensitivity. By contrast, spins initially prepared in a N00N state will evolve to $(|N0\rangle + e^{-iN\gamma_e Bt}|0N\rangle)/\sqrt{2}$ [15], thus providing a $\Delta B \propto 1/N$, HL-level sensitivity of B measurements.

IV. SUMMARY AND CONCLUSION

To summarize, we have shown that two entangled NVE quantum memories coupled to a superconducting qubit allow high-N00N states to be generated through a fast and robust procedure, involving just a few operational steps. A high immunity to decoherence is achieved through a reverse order of stages in N00N-state generation, with high-N Fock-state preparation in one of the NV ensembles preceding the stage at which the two NV memories are entangled. The proposed approach combines the key advantages of NV-diamond and circuit-QED quantum technologies, including the long coherence time of spins in NV centers, the capability of controlling NV centers by microwave and optical fields, the tunability of superconducting devices, and circuit scalability, thus providing an advantageous building block for quantum information and computation as well as quantum enhanced measurement technologies.

ACKNOWLEDGMENTS

This research was supported in part by the Welch Foundation (Grant No. A-1801) and the Russian Foundation for Basic Research (Project Nos. 16-02-00843 and 17-52-53092). Research into quantum optical physics and quantum technologies is supported by the Government of the Russian Federation (Project No. 14.Z50.31.0040, Feb. 17, 2017). Research into attosecond spectrochronography is supported by the Russian Science Foundation (Project No. 17-12-01533).

---

[1] B. P. Abbott *et al.*, Phys. Rev. Lett. **116**, 061102 (2016).
[2] T. Ono, R. Okamoto, and S. Takeuchi, Nat. Commun. **4**, 2426 (2013).
[3] V. Giovannetti, S. Lloyd, and L. Maccone, Science **306**, 1330 (2004).
[4] J. J. Bollinger, W. M. Itano, D. J. Wineland, and D. J. Heinzen, Phys. Rev A **54**, R4649 (1996).
[5] M. J. Holland and K. Burnett, Phys. Rev Lett. **71**, 1355 (1993).
[6] A. N. Boto, P. Kok, D. S. Abrams, S. L. Braunstein, C. P. Williams, and J. P. Dowling, Phys. Rev. Lett. **85**, 2733 (2000).
[7] B. C. Sanders, Phys. Rev. A **40**, 2417 (1989).
[8] J. P. Dowling, Contemp. Phys. **49**, 125 (2008).
[9] V. Giovannetti, S. Lloyd, and L. Maccone, Nat. Photon. **5**, 222 (2011).
[10] I. Afek, O. Ambar, and Y. Silberberg, Science **328**, 879 (2010).
[11] M. W. Mitchell, J. S. Lundeen, and A. M. Steinberg, Nature (London) **429**, 161 (2004).
[12] H. Wang, M. Hofheinz, M. Ansmann, R. C. Bialczak, E. Lucero, M. Neeley, A. D. O'Connell, D. Sank, J. Wenner, A. N. Cleland, and J. M. Martinis, Phys. Rev. Lett. **101**, 240401 (2008).
[13] M. Hofheinz, E. M. Weig, M. Ansmann, R. C. Bialczak, E. Lucero, M. Neeley, A. D. O'Connell, H. Wang, J. M. Martinis, and A. N. Cleland, Nature (London) **454**, 310 (2008).
[14] C. Guerlin, J. Bernu, S. Deleglise, C. Sayrin, S. Gleyzes, S. Kuhr, M. Brune, J. M. Raimond, and S. Haroche, Nature (London) **448**, 889 (2007).
[15] J. A. Jones, S. D. Karlen, J. Fitzsimons, A. Ardavan, S. C. Benjamin, G. A. D. Briggs, and J. J. L. Morton, Science **324**, 1166 (2009).
[16] H. Wang, M. Mariantoni, R. C. Bialczak, M. Lenander, E. Lucero, M. Neeley, A. D. O'Connell, D. Sank, M. Weides, J. Wenner, T. Yamamoto, Y. Yin, J. Zhao, J. M. Martinis, and A. N. Cleland, Phys. Rev. Lett. **106**, 060401 (2011).
[17] Q.-P. Su, C.-P. Yang, and S.-B. Zheng, Sci. Rep. **4**, 3898 (2014).
[18] D. Marcos, M. Wubs, J. M. Taylor, R. Aguado, M. D. Lukin, and A. S. Sørensen, Phys. Rev. Lett. **105**, 210501 (2010).
[19] W. Song, Z. Yin, W. Yang, X. Zhu, F. Zhou, and M. Feng, Sci. Rep. **5**, 7755 (2015).
[20] L. Childress, M. V. G. Dutt, J. M. Taylor, A. S. Zibrov, F. Jelezko, J. Wrachtrup, P. R. Hemmer, and M. D. Lukin, Science **314**, 281 (2006).
[21] M. G. Dutt, L. Childress, L. Jiang, E. Togan, J. Maze, F. Jelezko, A. S. Zibrov, P. R. Hemmer, and M. D. Lukin, Science **316**, 1312 (2007).
[22] I. V. Fedotov, L. V. Doronina-Amitonova, A. A. Voronin, A. O. Levchenko, S. A. Zibrov, D. A. Sidorov-Biryukov, A. B. Fedotov, V. L. Velichansky, and A. M. Zheltikov, Sci. Rep. **4**, 5362 (2014).
[23] X. Zhu, S. Saito, A. Kemp, K. Kakuyanagi, S. Karimoto, H. Nakano, W. J. Munro, Y. Tokura, M. S. Everitt, K. Nemoto, M. Kasu, N. Mizuochi, and K. Semba, Nature (London) **478**, 221 (2011).
[24] Z.-L. Xiang, S. Ashhab, J. Q. You, and F. Nori, Rev. Mod. Phys. **85**, 623 (2013).
[25] M. Reagor, W. Pfaff, C. Axline, R. W. Heeres, N. Ofek, K. Sliwa, E. Holland, C. Wang, J. Blumoff, K. Chou, M. J. Hatridge, L. Frunzio, M. H. Devoret, L. Jiang, and R. J. Schoelkopf, Phys. Rev. B **94**, 014506 (2016).
[26] N. Bar-Gill, L. M. Pham, A. Jarmola, D. Budker, and R. L. Walsworth, Nat. Commun. **4**, 1743 (2013).
[27] T. Liu, Q.-P. Su, S.-J. Xiong, J.-M. Liu, C.-P. Yang, and F. Nori, Sci. Rep. **6**, 32004 (2016).
[28] Z.-L. Xiang, X.-Y. Lu, T. F. Li, J. Q. You, and F. Nori, Phys. Rev. B **87**, 144516 (2013).
[29] X.-Y. Lü, Z.-L. Xiang, W. Cui, J. Q. You, and F. Nori, Phys. Rev. A **88**, 012329 (2013).
[30] K. Hammerer, A. S. Søensen, and E. S. Polzik, Rev. Mod. Phys. **82**, 1041 (2010).
[31] M. G. Raizen, R. J. Thompson, R. J. Brecha, H. J. Kimble, and H. J. Carmichael, Phys. Rev. Lett. **63**, 240 (1989).
[32] S. Saito, X. Zhu, R. Amsüss, Y. Matsuzaki, K. Kakuyanagi, T. Shimo-Oka, N. Mizuochi, K. Nemoto, W. J. Munro, and K. Semba, Phys. Rev. Lett. **111**, 107008 (2013).
[33] D.-W. Wang, H. Cai, R.-B. Liu, and M. O. Scully, Phys. Rev. Lett. **116**, 220502 (2016).
[34] N. Goldman and J. Dalibard, Phys. Rev. X **4**, 031027 (2014).
[35] G. Jotzu, M. Messer, R. Desbuquois, M. Lebrat, T. Uehlinger, D. Greif, and T. Esslinger, Nature (London) **515**, 237 (2014).
[36] D.-W. Wang, H. Cai, L. Yuan, S.-Y. Zhu, and R.-B. Liu, Optica **2**, 712 (2015).
[37] S. E. Nigg, Phys. Rev. A **89**, 022340 (2014).
[38] W. L. Yang, Y. Hu, Z. Q. Yin, Z. J. Deng, and M. Feng, Phys. Rev. A **83**, 022302 (2011).
[39] G. S. Agarwal, *Quantum Optics* (Cambridge University Press, Cambridge, 2013).
[40] W. L. Yang, Z.-q. Yin, Z. X. Chen, S.-P. Kou, M. Feng, and C. H. Oh, Phys. Rev. A **86**, 012307 (2012).
[41] W.-L. Song, W.-L. Yang, Z. Yin, C. Chen, and M. Feng, Sci. Rep. **6**, 33271 (2016).
[42] G. Balasubramanian *et al.*, Nature (London) **455**, 648 (2008).